JOURNAL OF VIROLOGY, Apr. 2006, p. 3607–3616 Vol. 80, No. 7
0022-538X/06/$08.00+0 doi:10.1128/JVI.80.7.3607–3616.2006

Mechanism of Substrate Recognition by Drug-Resistant Human Immunodeficiency Virus Type 1 Protease Variants Revealed by a Novel Structural Intermediate

Moses Prabu-Jeyabalan, Ellen A. Nalivaika, Keith Romano, and Celia A. Schiffer*

Department of Biochemistry and Molecular Pharmacology, University of Massachusetts Medical School, 364 Plantation Street, Worcester, Massachusetts 01605

Received 22 November 2005/Accepted 17 January 2006

Human immunodeficiency virus type 1 (HIV-1) protease processes and cleaves the Gag and Gag-Pol polyproteins, allowing viral maturation, and therefore is an important target for antiviral therapy. Ligand binding occurs when the flaps open, allowing access to the active site. This flexibility in flap geometry makes trapping and crystallizing structural intermediates in substrate binding challenging. In this study, we report two crystal structures of two HIV-1 protease variants bound with their corresponding nucleocapsid-p1 variant. One of the flaps in each of these structures exhibits an unusual "intermediate" conformation. Analysis of the flap-intermediate and flap-closed crystal structures reveals that the intermonomer flap movements may be asynchronous and that the flap which wraps over the P3 to P1 (P3-P1) residues of the substrate might close first. This is consistent with our hypothesis that the P3-P1 region is crucial for substrate recognition. The intermediate conformation is conserved in both the wild-type and drug-resistant variants. The structural differences between the variants are evident only when the flaps are closed. Thus, a plausible structural model for the adaptability of HIV-1 protease to recognize substrates in the presence of drug-resistant mutations has been proposed.

Maturation of human immunodeficiency virus type 1 (HIV-1) is achieved by the proteolytic processing of Gag and Gag-Pol sites at at least 10 nonhomologous substrate sites by a viral protease (4, 14, 36). This processing leads to the release of viral enzymes and structural proteins. In the absence of this proteolysis, immature noninfectious virions are produced (7). For this reason, HIV-1 protease is a prime target for antiviral therapy (48, 54).

The three-dimensional structure of this 22-kDa dimeric protease comprises a terminal region, an active site, and a core domain (29, 53). The active site residues are located at the dimer interface, with one catalytic aspartate (Asp25/25′) donated by each monomer (53, 54). The substrates bind the active site in an extended conformation forming mainly backbone hydrogen bonds (39, 51). On the opposite side of Asp25, two β-hairpins, known as the flaps, one from each monomer, wrap around the substrates. In addition to its interactions with the substrates, the flap tips (Ile50-Gly51) also participate in intermolecular interactions. As a common feature of aspartyl proteases for ligand binding to occur, several structural rearrangements must take place (13, 15, 24, 28, 45). The flaps open to allow substrate binding, and upon substrate recognition, they must close to attain the canonical "closed" conformation of HIV-1 protease. Whether the flap movements are synchronized between the monomers, as HIV-1 protease is homodimeric, or whether they move in an asynchronous fashion, as found in molecular dynamics simulations (22, 37, 45), is still to be verified structurally. The opening and the closing of the flaps are not likely random events but involve a few or several discrete structural intermediates. Nuclear magnetic resonance (NMR) experiments proposed that an ensemble of flap conformations are possible between open and closed stages of the flaps (12, 16). Whether other regions of the protease also move in concert with the flaps is not known. However, trapping any of these intermediates in a crystal is a challenge.

Our crystallographic investigations of wild-type (WT) and drug-resistant variants of HIV-1 protease complexed with several of its substrates have revealed a conserved shape we defined as the "substrate envelope," which we hypothesize is crucial for substrate specificity (39–42). Further studies provided structural insights into why a prime drug-resistant mutation, V82A (5, 8, 10, 31, 46), has less effect on substrate binding than on inhibitor binding as Val82 interacts more closely with the drugs than with natural substrates (41). The nucleocapsid-p1 (NC-p1) substrate, however, coevolves (AlaP2Val) in a correlated manner with the V82A mutation (3, 6, 9, 23, 56). Processing of the NC-p1 substrate is the slowest and rate-determining cleavage step in the maturation of Gag (38, 50, 55). Unlike in other substrate-V82A protease complexes, PheP1′ forms hydrophobic interactions with Val82, which are lost in the V82A complex (40). The AlaP2 in WT NC-p1 does not fill the S2 pocket, which is then compensated for by the ValP2 in the AP2V mutant (40). Thus, the AP2V coevolution in NC-p1 is structurally correlated by an interdependency between the P1′ and P2 substrate sites.

Here we report two new crystal structures of inactive D25N variants of HIV-1 protease bound to two variants of peptides corresponding to the NC-p1 cleavage site. Unlike the complexes of NC-p1 which were used to explain the coevolution of this substrate (40), these new structures exhibit a novel flap

* Corresponding author. Mailing address: Department of Biochemistry & Molecular Pharmacology, University of Massachusetts Medical School, 364 Plantation St., Worcester, MA 01605. Phone: (508) 856-8008. Fax: (508) 856-6464. E-mail: Celia.Schiffer@umassmed.edu.

TABLE 1. Crystallographic statistics of the two flap-intermediate NC-p1 complexes

Parameter	Structure[a]			
	$^{WT}NCp1_{WT\text{-}Int}$	($^{WT}NCp1_{WT}$)	$^{AP2V}NCp1_{V82A\text{-}Int}$	($^{AP2V}NCp1_{v82A}$)
Substrate sequence	RQAN*FLGKIN	(ERQAN*FLGKI)	RQVN*FLGKIN	(RQVN*FLGKIN)
Data collection				
Resolution (Å)	1.85	(2.1)	1.44	(2.0)
Space group	$P2_12_12_1$	($P2_12_12_1$)	$P2_12_12_1$	($P2_12_12_1$)
a (Å)	51.0	(51.1)	51.1	(50.8)
b (Å)	57.4	(57.7)	57.6	(57.3)
c (Å)	61.3	(61.5)	61.6	(60.9)
Z	4	(4)	4	(4)
Total no. of reflections	51,411	(38,149)	274,555	(80,252)
No. of unique reflections	14,812	(10,450)	33,155	(12,492)
R_{merge} (%)	5.6	(9.2)	4.7	(7.5)
Completeness (%)	92.7	(94.1)	100	(99.7)
I/σ_I	8.5	(4.5)	10.4	(9.0)
Crystallographic refinement				
R value (%)	19.5	(20.6)	18.7	(19.5)
R_{free} (%)	24.3	(23.3)	21.4	(23.1)
Sigma cutoff	None	(None)	None	(None)
RMSD in:				
Bond lengths (Å)	0.005	(0.004)	0.007	(0.005)
Bond angles (°)	1.0	(1.5)	1.3	(1.3)
PDB code	1FNS	(1TSU)	1FNT	(1TSQ)

[a] Statistics for the corresponding previously determined flap-closed complexes (40) are presented within parentheses.

conformation: One of the flaps remains in the canonical "flap-closed" geometry, while the other flap exhibits an unusual intermediate conformation. This is the first instance in which an asymmetric conformation of the flap is observed in HIV-1 protease. Detailed structural analyses provide a plausible structural model for how drug-resistant mutants continue to recognize substrates.

MATERIALS AND METHODS

Peptide acquisition. Two decameric peptides representing the P4-to-P6′ (P4-P6) region of the WT and AP2V variants of NC-p1 were purchased from 21st Century Biochemicals, Marlboro, Mass. (see Table 1 for sequence).

Nomenclature. To avoid confusion, the various crystal structures discussed here will use the following nomenclature: $^{(substrate\ variant)}substrate_{(protease\ variant)}$. For instance, WT D25N protease bound to WT NC-p1 with flaps in canonical and flap-intermediate conformations will be denoted by $^{WT}NCp1_{WT}$ and $^{WT}NCp1_{WT\text{-}Int}$, respectively.

Protein purification and crystallization. Mutagenesis, protein purification, and crystallization screens were carried out exactly as performed earlier (40).

Data collection. Data for $^{WT}NCp1_{WT\text{-}Int}$ were collected at the in-house Raxis IV image plate mounted on a Rigaku X-ray generator, and data for $^{AP2V}NCp1_{V82A\text{-}Int}$ were obtained from a synchrotron beam line at Advanced Light Source (ALS), Lawrence-Berkeley Laboratory, Berkeley, Calif. The WT and AP2V complexes diffracted to respective resolutions of 1.85 and 1.44 Å. Raw data were indexed using Denzo and scaled using ScalePack (30, 35), and the complete data collection statistics are listed in Table 1.

Structure solution and crystallographic refinement. The programs within the CCP4i interface (4a) were used throughout the crystallographic operations. The molecular replacement program AMoRe (34) was used to solve the structures using those reflections within the resolution range 12 to 3.5 Å. A WT HIV-1 protease complexed with the inhibitor TMC114 (Protein Data Bank [PDB] code 1T3R) (19) was used as the starting model. The phases were improved by building solvent molecules using ARP/wARP (32), and interactive model building was carried out using the graphics program O (17). Clear electron density for a different conformation was observed for the flap which interacts with the P1′-P6′ side of the substrate (Ile47′-Ile54′). Conjugate gradient refinement using Refmac5 (33) was performed by incorporating Schomaker and Trueblood tensor formulation of TLS (translation, libration, and screw rotation) parameters (21, 44b, 49). The interactive model building and crystallographic refinement were carried out iteratively until *R* and R_{free} converged. The final refinement statistics are presented in Table 1. The crystal coordinates have been deposited in the Protein Data Bank, and their accession codes are also listed in Table 1.

Structure analysis. (i) Structural superimpositions. All of the complexes used in this analysis were superimposed on the WT D25N complex of capsid-p2 peptide (PDB code 1F7A) (39). CA-$p2_{WT}$ was chosen in order to preserve consistency with all of our previous analyses. The terminal region (Pro1-Pro9 and Arg87-Phe99) from both monomers was used in this operation, and the superimposition was carried out such that the peptide orientation was preserved.

(ii) Double-difference plots. Distances between all the C_α atoms within each dimer were computed ($^nD_{ij}$, where D is the double difference and i and j are residue numbers). This was repeated for each of the "n" structures. Double differences (D) were generated as a ($i \times j$) matrix by computing the difference of the differences between the two dimers ($D = {}^nD_{ij} - {}^{n'}D_{ij}$). The ($i \times j$) matrix was then displayed as a contour diagram using GnuPlot (52).

RESULTS

Overall structure of protease. Crystal structures of WT and V82A variants of an inactive D25N HIV-1 protease enzyme were determined by cocrystallizing them with WT and AP2V variants of NC-p1 substrate peptide, respectively. The corresponding resolutions are 1.85 and 1.44 Å. The three-dimen-

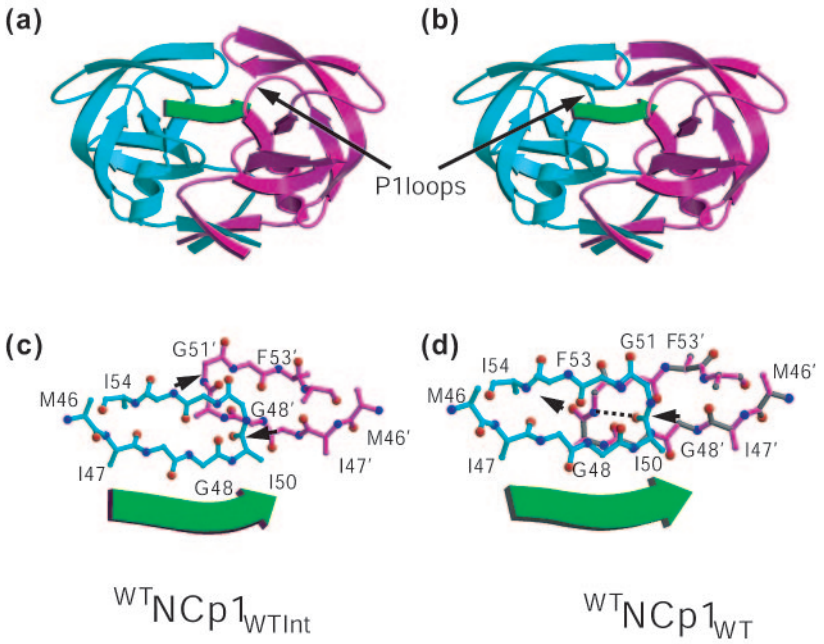

FIG. 1. (a and b) Crystal structures of $^{WT}NCp1_{WT\text{-}Int}$ and $^{WT}NCp1_{WT}$ (40). Monomers are distinguished in cyan and magenta, while the substrate is shown in green. This color scheme will be followed in most of the subsequent figures. (c) Stick representation of the flaps illustrating the conservation of direction of the Ile50 C = O group in the flap-intermediate arrangement. (d) Flap closure leads to the breakdown of dyad symmetry between the Ile50 C = O groups facilitating a conserved Ile50 N. . .O Gly51′ hydrogen bond. The direction of the C = O group is indicated by arrows. This figure and Fig. 3a and b and 5a and b were generated using Molscript (20).

sional arrangements of the terminal region forming the dimer interface, the active site region, and the core region, which is an extension of the active site, are all preserved as in other HIV-1 protease structures. The flap of the monomer which interacts with the P1′-P6′ side of the substrate (monomer B) exhibits a different geometry with the tip of the flap displaced by 4 Å. The flap of the monomer which interacts with the N-terminal side of the substrate (monomer A), on the other hand, adopts the usual flap geometry (Fig. 1). Other structures with semiopen flap conformation are symmetric (25, 44, 47); therefore, the two NC-p1 flap-intermediate structures represent a novel flap arrangement.

The method used to obtain the crystals of these flap-intermediate complexes is almost identical to the one followed in determining the corresponding flap-closed structures (40); in fact, the crystals were formed in the same crystallization tray. This conformation must represent an energetically stable form of the enzyme that can nucleate crystals similarly to the closed conformation. The exact reasons for this are unknown. Perhaps because NC-p1 is a poorer substrate (38, 50, 55), the binding of it is less strong, thus allowing for the possibility of more flap conformations to be accessed.

The root mean square deviations (RMSDs) for structural superposition were computed for all of the C_α atoms. The RMSD between $^{WT}NCp1_{WT\text{-}Int}$ and $^{AP2V}NCp1_{V82A\text{-}Int}$ is 0.22 Å, and the RMSD for $^{WT}NCp1_{WT}$ and $^{AP2V}NCp1_{V82A}$ is 0.53 Å. Thus, the structural agreement between the flap-intermediate complexes is better than it is between the flap-closed structures. The structural differences between the two flap-intermediate complexes were visualized by generating double-difference plots (Fig. 2a). Absence of significant peaks in the plot indicates that the structures of the two flap-intermediate complexes are similar. However, the $^{WT}NCp1_{WT}$ and $^{AP2V}NCp1_{V82A}$ complexes exhibit several relative shifts over 0.5Å (Fig. 2b). A comparison between $^{WT}NCp1_{WT\text{-}Int}$ and $^{WT}NCp1_{WT}$ also revealed several differences (Fig. 2c), with the flap of monomer B exhibiting the largest difference. The peaks (marked A1 and A2 in Fig. 2c) indicate the structural changes by the P1 loop (Gly78-Asn83) which pack closer to each other in the $^{WT}NCp1_{WT\text{-}Int}$ structure than in the corresponding final structures. The distance between the C_α atoms of Pro81 and Pro81′ is 1 Å shorter in $^{WT}NCp1_{WT\text{-}Int}$ than in $^{WT}NCp1_{WT}$ (Fig. 2e), which is also the case in comparing $^{AP2V}NCp1_{V82A\text{-}Int}$ and $^{AP2V}NCp1_{V82A}$ (Fig. 2e). The peaks (marked B1 and B2 in Fig. 2c) indicate a shortening of distance between the closed flap (of monomer A) and the P1 loops in $^{WT}NCp1_{WT\text{-}Int}$ (peaks marked B1 and B2 in Fig. 2c). Thus, the P1 loops are closest to AsnP1 and PheP1′ prior to complete closure of the flaps. As the flaps engage the substrates, the P1 loops relax open and move to their final position. The movements of P1 loops may hence be anticorrelated such that they contact the P1 and P1′ residues of the substrate and relax open as the flaps close down.

Crystal packing. Crystals for all four NC-p1 complexes grew in a $P2_12_12_1$ space group with similar unit cells (Table 1) and with one HIV-1 protease dimer in each asymmetric unit. The region around the flaps is not influenced by crystal packing in any of the complexes (Fig. 3). In fact, the residues in symmetry-related molecules, within 5Å of the flaps, do not change conformation between the complexes (Fig. 3c). There is enough space within the crystal lattice for either of the flaps to open. However, only the flap of monomer B adopts a flap-interme-

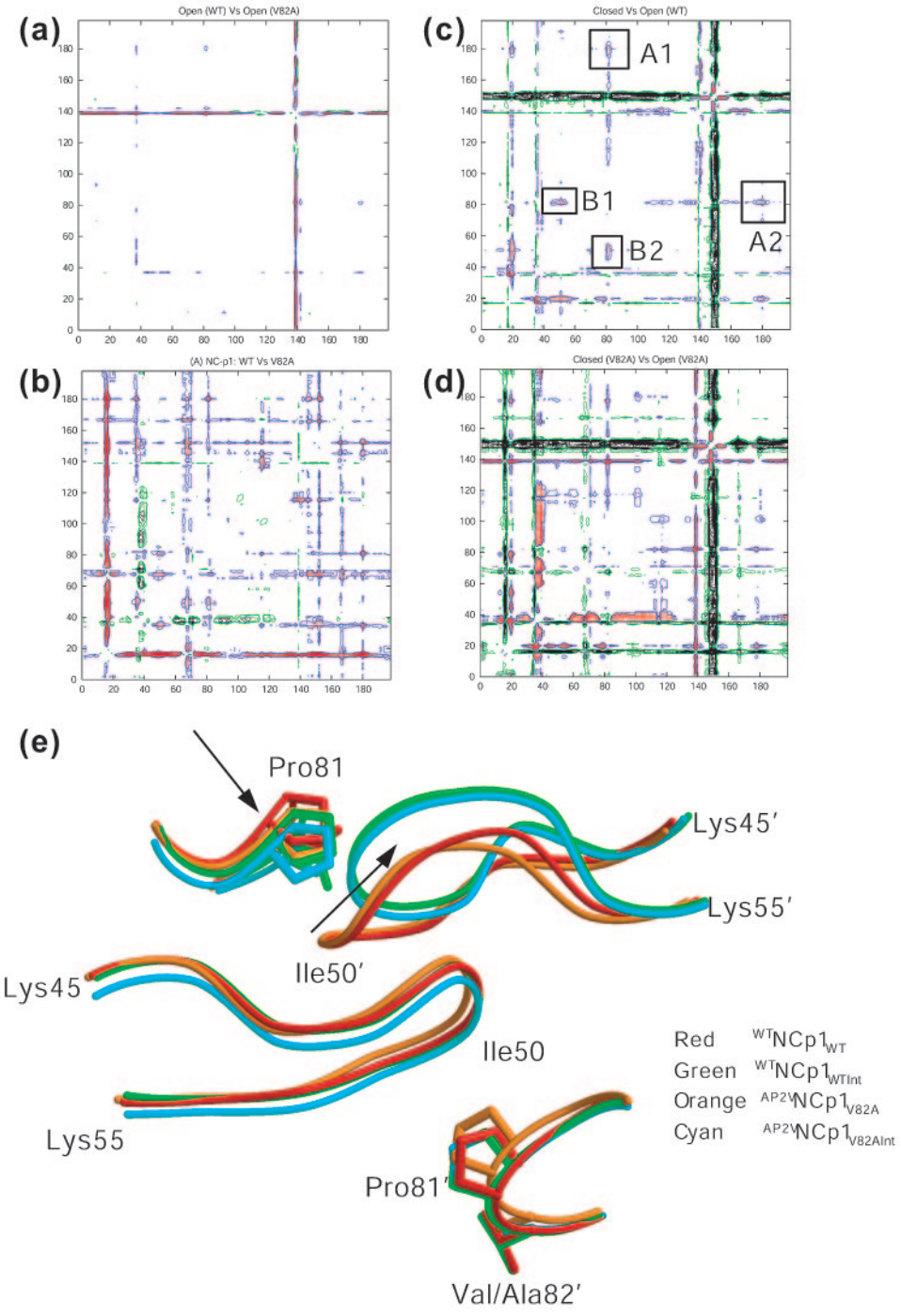

FIG. 2. Double-difference plots for (a) $^{WT}NCp1_{WT\text{-}Int}$ versus $^{AP2V}NCp1_{V82A\text{-}Int}$, (b) $^{WT}NCp1_{WT}$ versus $^{AP2V}NCp1_{V82A}$, (c) $^{WT}NCp1_{WT\text{-}Int}$ versus $^{WT}NCp1_{WT}$, and (d) $^{AP2V}NCp1_{V82A\text{-}Int}$ versus $^{AP2V}NCp1_{V82A}$. Panels were generated using GnuPlot (52). (e) Structural superposition of the P1 loops and the flaps for the four NC-p1 complexes: The movements of P1 loops are inversely correlated with respect to the flap movements as illustrated by the arrows. The color coding is as follows: red, $^{WT}NCp1_{WT}$; green, $^{WT}NCp1_{WT\text{-}Int}$; orange, $^{AP2V}NCp1_{V82A}$; cyan, $^{AP2V}NCp1_{V82A\text{-}Int}$. This panel and Fig. 3c, 4, and 5c and d were generated using MidasPlus (11).

diate conformation. These observations imply the following: the flap-intermediate geometry is not a crystallographic artifact; the flap interacting with P3-P1 residues may engage first; and the change in flap geometry could indeed be a discrete structural intermediate during substrate binding.

Flap conformation. Both of these complexes exhibit unambiguous electron density for the intermediate flap conformation (Fig. 3d). A comparison of the backbone (ϕ, ψ) angles with corresponding NC-p1 complexes exhibiting flap-closed arrangements reveals that the flap region of monomer B, en-

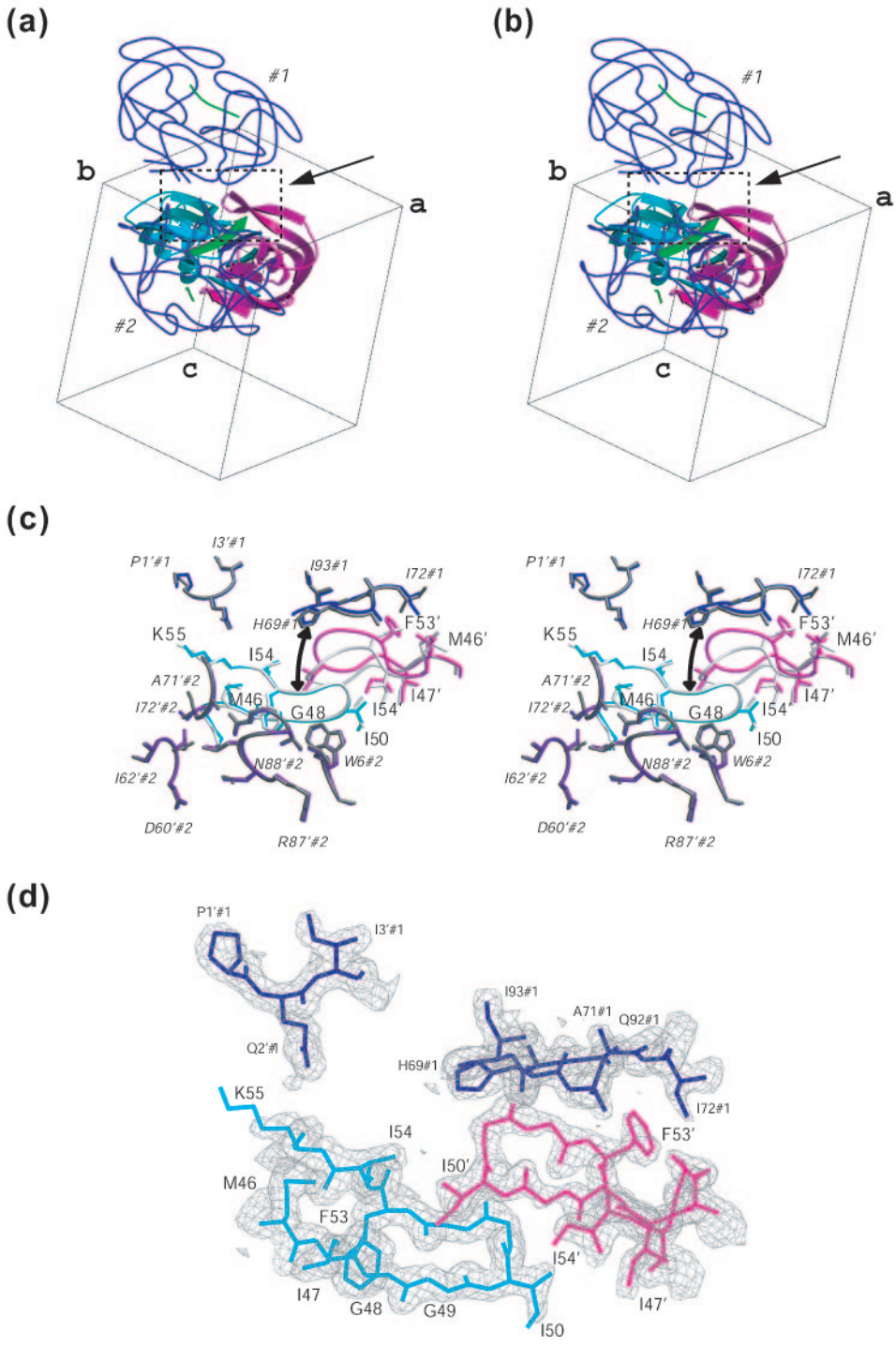

FIG. 3. Crystal packing diagrams of (a) $^{WT}NCp1_{WT\text{-}Int}$ and (b) $^{WT}NCp1_{WT}$ with the first and second symmetry operators of $P2_12_12_1$. The third symmetry is omitted as it does not form crystal contacts with the flaps. The boxed region with the arrow highlights the flap region, expanded in panel c. The color scheme is the same as Fig. 1, with the symmetry molecules in blue and the substrates in green. (c) Superimposed stereo diagram of the crystal packing of the flap region in $^{WT}NCp1_{WT\text{-}Int}$ (shown in cyan, magenta, blue, and purple) and $^{WT}NCp1_{WT}$ (shown in white and gray). The displacement of the flap of monomer B in $^{WT}NCp1_{WT\text{-}Int}$ is indicated by an arrow. (d) 2Fo-Fc electron density for the flaps and its surrounding region. The map was generated at a 1σ contour level, and for clarity, symmetry operator 2 has been omitted. The figure was generated using CHAIN (44a).

compassing Met46′-Ile54′, confers a sharp alteration in conformation (Ile47′, $\Delta\phi$ ~12° and $\Delta\psi$ ~20°; Gly48′, $\Delta\phi$ ~60° and $\Delta\psi$ ~140°; Phe53′, $\Delta\phi$ ~25° and $\Delta\psi$ ~180°; Ile54′, $\Delta\phi$ ~40° and $\Delta\psi$ ~20°) (Fig. 1a and c). Thus, there is a structural asymmetry between the flaps within the dimer; however, the carbonyl oxygens of Ile50 point toward each other in both monomers (ψ_{50} ~50° and ψ_{50}' ~50°) (Fig. 1c). In the flap-closed structure, the carbonyl oxygens of Ile50 and Ile50′ are

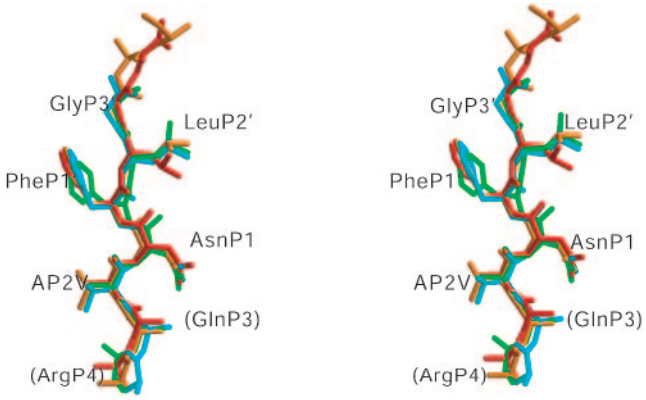

FIG. 4. Stereo diagram of superposition of substrate peptides from the four NC-p1 complexes. The substrate residues modeled as alanines due to lack of electron density are labeled within parentheses. See Fig. 2e for the color scheme.

asymmetric (ψ_{50} ~50° and ψ_{50}' ~138°) (Fig. 1d), thereby facilitating a highly conserved intermolecular hydrogen bonding pattern Ile50 O. . .N Gly51′ (or Ile50′ O. . .N Gly51) (Fig. 1d). The carbonyl oxygens pointing to each other in the flap-intermediate complex are the same as with the flap tip geometry observed in ligand-free flap-open structures (47), implying that the (ϕ, ψ) angles of the flap tips may be conserved between the monomers until complete flap closure is achieved.

Peptide conformation. The three-dimensional structure of the substrate peptides from both the flap-intermediate complexes is similar to the substrate structures in the flap-closed counterparts (Fig. 4). The substrates superimpose with RMSDs of 0.7 and 0.4 Å for the entire backbone and α-carbons, respectively. The only significant difference is the variability in orientation of the carbonyl oxygen of AsnP1 ($[\Delta\psi_{P1}]_{max}$ = 92°; $[\Delta\phi_{P1}']_{max}$ = 70°). As observed in the flap-closed NC-p1 complexes, however, the side chains of GlnP3 and ArgP4 are disordered. The peptide bond between AsnP1-PheP1′ in ^{AP2V}NCp1$_{V82A\text{-}Int}$ exhibits multiple conformations. Nevertheless, large structural alterations in the protease flap have not led to major changes in the peptide geometry, suggesting that the positioning of the substrates in a cleavable geometry may precede complete flap closure.

Substrate-protease hydrogen bonds. The substrate-protease hydrogen bonds are shown in Table 2. There are 11 substrate-protease hydrogen bonds in ^{WT}NCp1$_{WT\text{-}Int}$, and there are 13 and 15 substrate-protease hydrogen bonds for the two substrate peptide conformations in ^{AP2V}NCp1$_{V82A\text{-}Int}$. In both of the complexes, AsnP1 ND2 makes a hydrogen bond to Gly27 O (Fig. 5a). This hydrogen bond, which is also found in ^{AP2V}NCp1$_{V82A}$ (Fig. 5b), is a unique interaction of the NC-p1 substrate in which the side chain of a P1 residue forms a direct hydrogen bond. The flap residue Gly48 forms backbone hydrogen bonds with the P4-P1 side of the substrate, while Gly48′ does not form hydrogen bonds with the P1′-P6′ side due to the flap movement (Fig. 5a). Despite flap movement, however, the P1′-P6′ side forms conserved hydrogen bonds with Gly27′ O and Asp29′ N. The substrate-protease hydrogen bonds in the flap-intermediate complexes were compared with those in the corresponding flap-closed complexes (Fig. 5b). Ten hydrogen bonds are conserved between ^{WT}NCp1$_{WT}$ and ^{AP2V}NCp1$_{V82A}$, which include the 4 formed by the flap residue Gly48/Gly48′ (Table 2). Of these 10 conserved hydrogen bonds, 7 and 8 are

TABLE 2. Substrate-protease hydrogen bonds[a]

Substrate	Protease	Bonding result for:[b]			
		^{WT}NCp1$_{WT\text{-}Int}$	^{WT}NCp1$_{WT}$	^{AP2V}NCp1$_{V82A\text{-}Int}$	^{AP2V}NCp1$_{V82A}$
P4 N	Asp29 OD2	2.9			
P4 N	Asp30 OD2	3.3			2.9
P4 O	Asp30 OD2	3.0			
P4 O	**Gly48 N**		**3.2**	**2.7**	**3.0**
P3 N	**Asp29 OD2**	**3.0**	**3.5**	**3.2**	**3.3**
P3 O	**Asp29 N**	**2.9**	**3.6**	**3.0**	**2.8**
P2 N	**Gly48 O**	**2.9**	**3.2**	**2.8**	**2.8**
P1 N	**Gly27 O**	**3.2**	**3.2**	**3.2 (3.1)**	**2.8**
P1 ND2	Gly27 O	3.4		3.3	3.5
P1 O	Asn25′ ND2			(3.1)	
P1 O	Asn25 OD1			(3.1)	
P1 O	Asn25 ND2			(3.2)	
P1 O	Asn25′ OD1			(3.3)	
P1 O	**Asn25′ ND2**	**3.3**	**3.2**	**2.8**	**2.5**
P2′ N	**Gly27′ O**	**3.1**	**3.2**	**3.0 (3.1)**	**2.9**
P2′ O	**Asp29′ N**	**3.0**	**3.1**	**3.0 (3.0)**	**2.9**
P3′ N	Gly48′ O		**3.1**		**2.8**
P3′ O	Gly48′ N		**3.1**		**2.8**
P3′ O	Arg8 NH2			3.4	
P3′ O	Asp29′ OD2			3.2	
				3.3	
				3.5	
P4′ N	Asp29′ OD2		**3.6**		**3.0**

[a] Donor-acceptor distances within 3.6 Å were treated as hydrogen bonds if the angles of N-H...O and C-O...O interactions were greater than 120° and greater than 90°, respectively.

[b] Hydrogen bonding distances for a second conformation of the peptide in ^{AP2V}NCp1$_{V82A\text{-}Int}$ are presented within parentheses. Hydrogen bonds conserved in all substrate-protease complexes (42) are highlighted in bold.

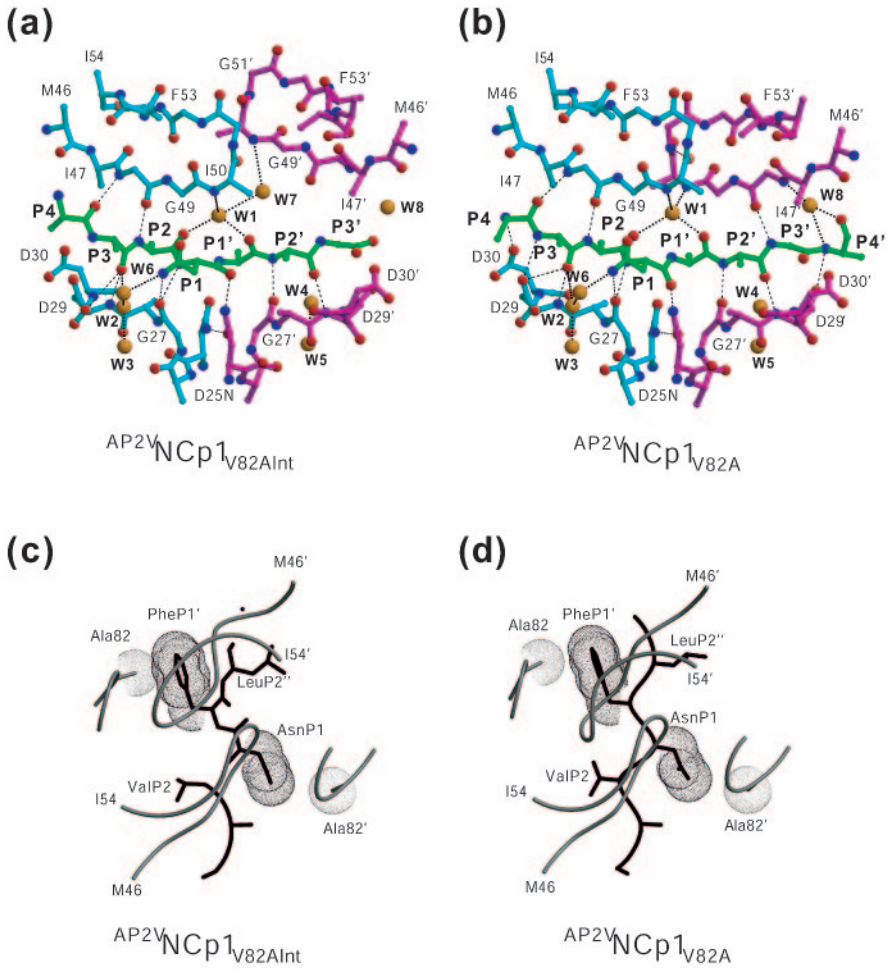

FIG. 5. Illustration of the substrate-protease hydrogen bonds in (a) $^{AP2V}NCp1_{V82A\text{-}Int}$ and (b) $^{AP2V}NCp1_{V82A}$. Monomers are distinguished in cyan and magenta, while the substrate is shown in green. Oxygens and nitrogens are illustrated as red and blue balls, respectively, and water molecules are shown as orange hard spheres. Hydrogen bonds and water bridges are shown by dotted lines. The VDW interaction between Ala82 and the substrates in panels c ($^{AP2V}NCp1_{V82A\text{-}In}$) and d ($^{AP2V}NCp1_{V82A}$) is illustrated as viewed down the molecular dyad axis. The protease and substrate models are shown in gray and black, respectively. VDW surfaces are shown for the side chain atoms of Ala82, AsnP1, and PheP1′.

present in $^{WT}NCp1_{WT\text{-}Int}$ and $^{AP2V}NCp1_{V82A\text{-}Int}$, respectively, with comparable hydrogen bonding distances. Barring hydrogen bonds by Gly48′, the alteration in flap geometry has less influence on substrate-protease hydrogen bonds.

Water-mediated substrate-protease bridges. The active site waters which are conserved among other HIV-1 protease-substrate complexes (2, 26, 46) are also present in the NC-p1 flap-intermediate complexes (labeled W1 to W5 in Fig. 5a and b). The water site W1, which coordinates Ile50/50′ N and P2 O and P1′ O in a tetrahedral geometry in most flap-closed structures, is also observed in the flap-intermediate structures, despite changes in the flap conformation. This water is stabilized by another water, W7, which mimics the position of Ile50′ N in the flap-intermediate conformation and bridges W1 with the new Ile50′ N, thereby preserving the geometry (Fig. 5a). Two waters, W6 and W8, have unique geometries in all of the NC-p1 complexes. W6 bridges AsnP1 ND2 with Gly27 O, while W8 mediates GlyP3′ O to Gly48′ N in the flap-intermediate complexes and P4′ O to Gly48′ N in the flap-closed complexes. Thus, the water bridging network between the flap-intermediate and the flap-closed structures, for the most part, is also preserved.

van der Waals interactions. The side chain to side chain van der Waals (VDW) contacts between the substrate peptide and protease for all four NC-p1 complexes are summarized in Table 3. In both WT complexes, AlaP2, the AP2V substrate mutation site, makes a lone VDW interaction. The valine mutation in the V82A-AP2V complexes enables ValP2 to form five and nine contacts, all hydrophobic, in $^{AP2V}NCp1_{V82A\text{-}Int}$ and $^{AP2V}NCp1_{V82A}$, respectively. The major contributor to the loss of four VDW contacts in $^{AP2V}NCp1_{V82A\text{-}Int}$ is the alteration of the flap in monomer B, suggesting complete flap closure will stabilize the P2 residue. In the flap-intermediate complexes, the residues involved in VDW interactions with LeuP2′, Ala28′ and Val32′, are conserved; however, upon flap closure, Ile50 and Ile47′ also contact LeuP2′ (Table 3). The structures of GlyP3′ and its VDW contacts (with Arg8 and Asp29′) are highly conserved among the four NC-p1 complexes.

The numbers of VDW contacts made by AsnP1 are similar between the two flap-intermediate structures, while they are

TABLE 3. Summary of side-chain-related substrate-protease van der Waals interactions[a]

Type of side chain contact	Result for			
	$^{WT}NCp1_{WT\text{-}Int}$	$^{WT}NCp1_{WT}$	$^{AP2V}NCp1_{V82A\text{-}Int}$	$^{AP2V}NCp1_{V82A}$
(ArgP4)[b]				
Protease residues		I47, D30	D29, D30	D29, D30
Total contacts		4	2	2
Hydrophobic contacts	0	3	0	0
(GlnP3)[b]				
Protease residues	D29, R8′		D29, R8′	D29, R8′
Total contacts	2		2	2
Hydrophobic contacts	0	0	0	0
AlaP2/ValP2				
Protease residues	A28	A28	A28, V32 I47	A28, V32, I47 I84, I50′
Total contacts	1	1	5	9
Hydrophobic contacts	1	1	5	9
AspP1				
Protease residues	L23, G49, N25′ P81′, V82′, I84′	L23, N25′ P81′, V82′, I84′	L23, G49, N25′ P81′, I84′	L23, G49, N25′ P81′, I84′
Total contacts	10	11	9	7
Hydrophobic contacts	3	3	2	1
Contacts by P1 loop	7	9	6	4
PheP1′				
Protease residues	N25, P81, V82 I84, L23′, G27′	R8, N25, P81 V82, I84, L23′	N25, P81, A82 I84, L23′	N25, P81, I84 L23′, G49′
Total contacts	15	13	11	9
Hydrophobic contacts	13	10	10	8
Contacts by P1 loop	10	8	8	5
Contacts by Val82/Ala82	5	5	4	0
LeuP2′				
Protease residues	A28′, D30′, V32′	I50, A28′, V32′ I47′, I84′	A28′, V32′	I50, A28′, V32′ I47′
Total contacts	6	9	4	9
Hydrophobic contacts	5	9	4	9
GlyP3′				
Protease residues	R8, D29′	R8, D29′	R8, D29′	R8, D29′
Total contacts	3	3	3	2
Hydrophobic contacts	1	1	1	0

[a] A distance criterion of 4.2 Å was used to compute the VDW contacts.
[b] Modeled as alanines due to lack of electron density.

significantly different between the two flap-closed complexes (Table 3). Presumably, the V82A mutation is responsible for most of the loss in VDW contacts in $^{AP2V}NCp1_{V82A}$ (total contacts, 7; 4 by the P1 loop) compared to $^{WT}NCp1_{WT}$ (total contacts, 11; 7 by the P1 loop). However, in $^{AP2V}NCp1_{V82A\text{-}Int}$, the P1 loop shifts toward the center of the dimer packing against AsnP1 (total contacts, nine; six by the P1 loop), regaining some additional VDW interactions.

The most significant changes in VDW interactions are exhibited by PheP1′. In both WT complexes, Val82 forms five VDW interactions which are lost in $^{AP2V}NCp1_{V82A}$ due to the V82A mutation. In $^{AP2V}NCp1_{V82A\text{-}Int}$, however, Ala82 CB participates in four VDW interactions (Table 3 and Fig. 5c). As in $^{AP2V}NCp1_{V82A\text{-}Int}$, the P1 loop forms more contacts with PheP1′ in $^{WT}NCp1_{WT\text{-}Int}$ (10 contacts) than in $^{WT}NCp1_{WT}$ (8 contacts). The participation of Ala82 in substrate-protease VDW interaction prior to complete flap closure suggests two interrelated scenarios. (i) Residue 82 forms VDW contacts with the substrate prior to flap closure regardless of amino acid type (Fig. 5c). (ii) Upon flap closure, residue 82, a member of the P1 loop, moves away from the active site (Fig. 5d), thus altering substrate-protease VDW interactions.

DISCUSSION

The results of the two flap-intermediate NC-p1 complexes emphasize two aspects of substrate recognition by HIV-1 protease. (i) The flap interacting with the P4-P1 side of the substrate closes first, thereby reiterating our hypothesis that P3-P1 residues are crucial for substrate recognition. (ii) The P1 loops move toward the P1 and P1′ residues of the substrates prior to flap closure, and upon flap closure the P1 loops relax open toward their final position. In addition, the flap-intermediate structures presented here are very similar in structure (Fig. 2a), suggesting that these structures are not a random conformation but represent a highly conserved discrete structural inter-

mediate. This is consistent with results obtained from NMR studies (12, 16), and therefore a discrete structural intermediate in substrate recognition by HIV-1 protease has been trapped.

Both of the flaps in the dimer could potentially assume an intermediate geometry within this crystal form; however, only the flap interacting with the P4-P1 side of the substrate adopts a closed conformation, implying that the P3-P1 region of the substrate may be crucial for specificity (1, 27, 42). The crystal structure of HIV-1 protease product complex retains only the P5-P1 side (Ac-Ser-Leu-Asn-Phe/) of the substrate Ac-Ser-Leu-Asn-Phe*Phe-Leu-Glu-Lys (PDB code 1YTH) (43). This product complex further supports our claim that the P3-P1 side of the substrate is bound more stably.

The analysis of VDW interactions elucidates the intricate involvement of P1 loop in substrate binding prior to and after flap closure in substrate recognition. While the flaps are in transition, the P1 loops act as guides by supplying the necessary packing interaction to the substrate, especially to P1 and P1′. Ala82 contacts PheP1′ in the flap-intermediate conformation (Fig. 5c), while in the flap-closed structures, it moves away, resulting in loss of VDW contacts (Fig. 5d), which implies that during initial stages of substrate recognition, the P1 and P1′ sites make more VDW contacts than when the flaps are engaged. The P2 and P2′ residues, however, require complete flap closure for optimal binding. This is consistent with why coevolution should take place at the P2 site in the NC-p1 substrate in response to the V82A protease mutation.

The inward movement of the P1 loop when the flaps adopt an intermediate conformation could be general for all WT and V82A variants of HIV-1 protease. We have also observed this flap-intermediate conformation in the crystal structure of a multidrug-resistant HIV protease variant (L10I/G48V/I54V/L63P/V82A) complexed with nelfinavir (NFV) (unpublished data). This NFV complex also crystallized in the same space group as the NC-p1 structures with similar unit cell dimensions. The conformation of the flaps and the P1 loops of this NFV complex is the same as that of the NC-p1 flap-intermediate structures. More importantly, the positioning of the inhibitor NFV tilts by ~15° about the molecular dyad compared to NFV in the wild-type complex, presumably in a nonoptimal conformation (18). In contrast, the substrates in the flap-intermediate complexes form a stable geometry which is ready for cleavage even in the intermediate state (Fig. 4).

In light of the data presented, we postulate a structural mechanism for substrate recognition that occurs regardless of the presence or absence of drug-resistant mutations. Prior to flap closure, the substrate is already bound in an extended form and the substrate-protease VDW interactions are preserved in both the WT and drug-resistant protease variants. When the flaps close, the mutation sites move to their final positions, thereby impacting the efficient binding of inhibitors but not the binding of substrates. These flap-intermediate structures thus open a new dimension into the molecular knowledge of the adaptability of drug-resistant protease mutants.

ACKNOWLEDGMENTS

The authors thank Nancy King for useful suggestions and Tuba Bas, Balaji Bhyravbhatla, and Luca Leone for experimental and technical assistance. Synchrotron data were collected at Advanced Light Source, Lawrence-Berkeley Laboratory, Berkeley, Calif., with the help of Nick Sauter.

This work is funded by National Institutes of Health grant RO1 GM64347-05.

REFERENCES

1. **Andersson, H. O., K. Fridborg, S. Lowgren, M. Lalterman, A. Muhlman, M. Bjorsne, N. Garg, I. Kyarnstrom, W. Schaal, B. Classon, A. Karlen, U. H. Danielson, G. Ahlsen, U. Nillroth, L. Vrang, B. Oberg, B. Samuelsson, A. Hallberg, and T. Unge.** 2003. Optimization of P1-P3 groups in symmetric and asymmetric HIV-1 protease inhibitors. Eur. J. Biochem. **270:**1756–1758.
2. **Baldwin, E. T., T. N. Bhat, S. Gulnik, B. Liu, I. A. Topol, Y. Kiso, T. Mimoto, H. Mitsuya, and J. W. Erickson.** 1995. Structure of HIV-1 protease with KNI-272, a tight-binding transition-state analog containing allophyenylnorstatine. Structure **3:**581–590.
3. **Bally, F., R. Martinez, S. Peters, P. Sudre, and A. Telenti.** 2000. Polymorphism of HIV type 1 Gag p7/p1 and p1/p6 cleavage sites: clinical significance and implications for resistance to protease inhibitors. AIDS Res. Hum. Retrovir. **16:**1209–1213.
4. **Chou, K.** 1996. Prediction of human immunodeficiency virus protease cleavage sites in proteins. Anal. Biochem. **233:**1–14.

4a. **Collaborative Computational Project Number 4.** 1994. The CCP4 suite: programs for protein crystallography. Acta Crystallogr. Sect. D Biol. Crystallogr. *D***50:**760–763.

5. **Condra, J. H., W. A. Schleif, O. M. Blahy, L. J. Gabryelski, D. J. Graham, J. C. Quintero, A. Rhodes, H. L. Robbins, E. Roth, M. Shivaprakash, D. Titus, T. Yang, H. Teppler, K. E. Squires, P. J. Deutsch, and E. Emini.** 1995. *In vivo* emergence of HIV-1 variants resistant to multiple protease inhibitors. Nature **374:**569–571.
6. **Côté, H. C. F., Z. L. Brumme, and P. R. Harrigan.** 2001. Human immunodeficiency virus type 1 protease cleavage site mutations associated with protease inhibitor cross-resistance selected by indinavir, ritonavir, and/or saquinavir. J. Virol. **75:**589–594.
7. **Darke, P. L., R. F. Nutt, S. F. Brady, V. M. Garsky, T. M. Ciccarone, C. T. Leu, P. K. Lumma, R. M. Freidinger, D. F. Vebal, and I. S. Sigal.** 1988. HIV-1 protease specificity of peptide cleavage is sufficient for processing of *gag* and *pol* polyproteins. Biochem. Biophys. Res. Commun. **156:**297–303.
8. **Deeks, S. G., R. M. Grant, G. W. Beatty, C. Horton, J. Detmer, and S. Eastman.** 1998. Activity of a ritonavir plus saquinavir-containing regimen in patients with virologic evidence of indinavir or ritonavir failure. AIDS Res. Hum. Retrovir. **12:**F97–F102.
9. **Doyon, L., G. Croteau, D. Thibeault, F. Poulin, L. Pilote, and D. Lamarre.** 1996. Second locus involved in human immunodeficiency virus type 1 resistance to protease inhibitors. J. Virol. **70:**3763–3769.
10. **Eastman, P. S., J. Mittler, R. Kelso, C. Gee, E. Boyer, J. Kolberg, M. Urdea, J. M. Leonard, D. W. Norbeck, H. Mo, and M. Markowitz.** 1998. Genotypic changes in human immunodeficiency virus type 1 associated with loss of suppression of plasma viral RNA levels in subjects treated with ritonavir (Norvir) monotherapy. J. Virol. **72:**5154–5164.
11. **Ferrin, T. E., C. C. Huang, L. E. Jarvis, and R. Langridge.** 1988. The MIDAS display system. J. Mol. Graphics **6:**13–27.
12. **Freedberg, D. I., R. Ishima, J. Jacob, Y. X. Wang, I. Kustanovich, J. M. Louis, and D. A. Torchia.** 2002. Rapid structural fluctuations of the free HIV protease flaps in solution: relationship to crystal structures and comparison with predictions of dynamics calculations. Protein Sci. **11:**221–232.
13. **Groves, M. R., V. Dhanaraj, M. Badasso, P. Nugent, J. E. Pitts, D. J. Hoover, and T. L. Blundell.** 1998. A 2.3 Å resolution structure of chymosin complexed with a reduced bond inhibitor shows that the active site β-hairpin flap is rearranged when compared with the native crystal structure. Protein Eng. **10:**833–840.
14. **Henderson, L. E., T. D. Copeland, R. C. Sowder, A. M. Schultz, and S. Oraszlan.** 1988. Human retroviruses, cancer and AIDS: approaches to prevention and therapy. Liss, New York, N.Y.
15. **Hong, L., and J. Tang.** 2004. Flap position of free memapsin 2 (β-secretase), a model for flap opening in aspartic protease catalysis. Biochemistry **43:**4689–4695.
16. **Ishima, R., D. I. Freedberg, Y. X. Wang, J. M. Louis, and D. A. Torchia.** 1999. Flap opening and dimer-interface flexibility in the free and inhibitor-bound HIV protease, and their implications for function. Structure Fold. Des. **7:**1047–1055.
17. **Jones, T. A., M. Bergdoll, and M. Kjeldgaard.** 1990. O: a macromolecular modeling environment, p. 189–195. *In* C. Bugg and S. Ealick (ed.), Crystallographic and modeling methods in molecular design. Springer-Verlag Press, Berlin, Germany.
18. **Kaldor, S., V. Kalish, J. N. Davies, B. Shetty, J. Fritz, K. Appelt, J. Burgess, K. Campanale, N. Chirgadze, D. K. Clawson, B. A. Dressman, S. D. Hatch, D. A. Khalil, M. B. Kosa, P. P. Lubbehusen, M. A. Muesing, A. K. Patick, S. H. Reich, K. S. Su, and J. H. Tatlock.** 1997. Viracept (nelfinavir mesylate, AG1343): a potent, orally bioavailable inhibitor of HIV-1 protease. J. Med. Chem. **40:**3979–3985.

19. **King, N. M., M. Prabu-Jeyabalan, E. A. Nalivaika, P. Wigerinck, M.-P. de Bethune, and C. A. Schiffer.** 2004. Structural and thermodynamic basis for the binding of TMC114, a next-generation human immunodeficiency virus type 1 protease inhibitor. J. Virol. **78:**12012–12021.
20. **Kraulis, P. J.** 1991. Molscript: a program to produce both detailed and schematic plots of protein structures. J. Appl. Crystallogr. **24:**946–950.
21. **Kuriyan, J., and W. I. Weis.** 1991. Rigid protein motion as a model for crystallographic temperature factors. Proc. Natl. Acad. Sci. USA **88:**2773–2777.
22. **Kurt, N., W. R. P. Scott, A. C. Schiffer, and T. Haliloglu.** 2003. Cooperative fluctuations of unliganded and substrate-bound HIV-1 protease: a structure-based analysis on a variety of conformations from crystallography and molecular dynamics simulations. Proteins Struct. Funct. Genet. **51:**409–422.
23. **La Seta Catamoncio, S., M. P. De Pasquale, P. Citterio, S. Kurtagic, M. Galli, and S. Rusconi.** 2001. *In vitro* evolution of the human immunodeficiency virus type 1 Gag-protease region and maintenance of reverse transcriptase resistance following prolonged drug exposure. J. Clin. Microbiol. **39:**1124–1129.
24. **Lee, A. Y., S. V. Gulnick, and J. W. Erickson.** 1998. Conformational switching in aspartic proteinase. Nat. Struct. Biol. **5:**866–871.
25. **Logsdon, B. C., J. F. Vickrey, P. Martin, G. Proteasa, J. I. Koepke, S. R. Terlecky, Z. Wawrzak, M. A. Winters, T. C. Merigan, and L. C. Kovari.** 2004. Crystal structures of a multidrug-resistant human immunodeficiency virus type 1 protease reveal an expanded active-site cavity. J. Virol. **78:**3123–3132.
26. **Mahalingam, B., J. M. Louis, J. Hung, R. W. Harrison, and I. T. Weber.** 2001. Structural implications of drug-resistant mutants of HIV-1 protease: high-resolution crystal structures of the mutant protease/substrate analogue complexes. Proteins **43:**455–464.
27. **Martin, J. L., J. Begun, A. Schindeler, W. A. Wickramasinghe, D. Alewood, P. F. Alewood, D. A. Bergman, R. I. Brinkworth, G. Abbenante, D. R. March, R. C. Reid, and D. P. Fairlie.** 1999. Molecular recognition of macrocyclic peptidomimetic inhibitors by HIV-1 protease. Biochemistry **38:**7978–7988.
28. **Meagher, K. L., and H. A. Carlson.** 2005. Solvation influences flap collapse in HIV-1 protease. Proteins Struct. Funct. Genet. **58:**119–125.
29. **Miller, M., J. Schneider, B. K. Sathyanarayana, M. V. Toth, G. R. Marshall, L. Clawson, L. Selk, S. B. Kent, and A. Wlodawer.** 1989. Structure of complex of synthetic HIV-1 protease with a substrate-based inhibitor at 2.3-Å resolution. Science **246:**1149–1152.
30. **Minor, W.** 1993. XDISPLAYF program. Purdue University, West Lafayette, Ind.
31. **Molla, A., M. Korneyeva, Q. Gao, S. Vasavanonda, P. Schipper, H. Mo, M. Markowitz, T. Chernyavskiy, P. Niu, N. Lyons, A. Hsu, G. Granneman, D. Ho, C. Boucher, J. Leonard, D. Norbeck, and D. Kempf.** 1996. Ordered accumulation of mutations in HIV protease confers resistance to ritonavir. Nat. Med. **2:**760–766.
32. **Morris, R. J., A. Perrakis, and V. S. Lamzin.** 2002. ARP/wARP's model-building algorithms. I. The main chain. Acta Crystallogr. Sect. D Biol. Crystallogr. *D***58:**968–975.
33. **Murshudov, G. N., A. A. Vagin, and E. J. Dodson.** 1997. Refinement of macromolecular structures by the maximum-likelihood method. Acta Crystallogr. Sect. D Biol. Crystallogr. *D***53:**240–255.
34. **Navaza, J.** 1994. AMoRe: an automated package for molecular replacement. Acta Crystallogr. Sect. D Biol. Crystallogr. *A***50:**157–163.
35. **Otwinowski, Z., and W. Minor.** 1997. Processing of X-ray diffraction data collected in oscillation mode. Methods Enzymol. **276:**307–326.
36. **Peng, C., B. K. Ho, T. W. Chang, and N. T. Chang.** 1989. Role of human immunodeficiency virus type 1-specific protease in core protein maturation and viral infectivity. J. Virol. **63:**2550–2556.
37. **Perryman, A. L., J.-H. Lin, and A. McCammon.** 2004. HIV-1 protease molecular dynamics of a wild-type and of the V82F/I84V mutant: possible contributions to drug resistance and a potential new target site for drugs. Protein Sci. **13:**1108–1123.
38. **Pettit, S. C., N. Sheng, R. Tritch, S. Erickson-Vitanen, and R. Swanstrom.** 1998. The regulation of sequential processing of HIV-1 Gag by the viral protease. Adv. Exp. Med. Biol. **436:**15–25.
39. **Prabu-Jeyabalan, M., E. Nalivaika, and C. A. Schiffer.** 2000. How does a symmetric dimer recognize an asymmetric substrate? A substrate complex of HIV-1 protease. J. Mol. Biol. **301:**1207–1220.
40. **Prabu-Jeyabalan, M., E. A. Nalivaika, N. M. King, and C. A. Schiffer.** 2004. Structural basis for coevolution of a human immunodeficiency virus type 1 nucleocapsid-p1 cleavage site with a V82A drug-resistant mutation in viral protease. J. Virol. **78:**12446–12454.
41. **Prabu-Jeyabalan, M., E. A. Nalivaika, N. M. King, and C. A. Schiffer.** 2003. Viability of a drug-resistant human immunodeficiency virus type 1 protease variant: structural insights for better antiviral therapy. J. Virol. **77:**1306–1315.
42. **Prabu-Jeyabalan, M., E. A. Nalivaika, and C. A. Schiffer.** 2002. Substrate shape determines specificity of recognition for HIV-1 protease: analysis of crystal structures of six substrate complexes. Structure **10:**369–381.
43. **Rose, R. B., C. S. Craik, N. L. Douglas, and R. M. Stroud.** 1996. Three-dimensional structures of HIV-1 and SIV protease product complexes. Biochemistry **35:**12933–12944.
44. **Rose, R. B., C. S. Craik, and R. M. Stroud.** 1998. Domain flexibility in retroviral proteases: structural implications for drug resistant mutations. Biochemistry **37:**2607–2621.

44a. **Sack, J. S.** 1998. CHAIN—a crystallographic modeling program. J. Mol. Graphics **6:**224–225.

44b. **Schomaker, V., and K. N. Trueblood.** 1968. On the rigid-body motion of molecules in crystals. Acta Crystallogr. Sect. B **24:**63–76.

45. **Scott, W. R. P., and C. A. Schiffer.** 2000. Curling of flap tips in HIV-1 protease as a mechanism for substrate entry and tolerance of drug resistance. Structure **8:**1259–1265.
46. **Shafer, R. W., D. Stevenson, and B. Chan.** 1999. Human immunodeficiency virus reverse transcriptase and protease sequence database. Nucleic Acids Res. **27:**348–352.
47. **Spinelli, S., Q. Z. Liu, P. M. Alzari, P. H. Hirel, and R. J. Poljak.** 1991. The three-dimensional structure of the aspartyl protease from the HIV-1 isolate BRU. Biochimie **73:**1391–1396.
48. **Temesgen, Z.** 2001. Current status of antiretroviral therapies. Expert Opin. Pharmacother. **2:**1239–1246.
49. **Tickle, I. J., and D. S. Moss.** 1999. Modelling rigid-body thermal motion in macromolecular crystal structure refinement. IUCr99 Computing School, London, United Kingdom. [Online.] http://people.cryst.bbk.ac.uk/~tickle/iucr99/.
50. **Tözsér, J., I. Blaha, T. D. Copeland, E. M. Wondrak, and S. Oroszlan.** 1991. Comparison of the HIV-1 and HIV-2 proteinases using oligopeptide substrate representing cleavage sites in Gag and Gag-Pol polyproteins. FEBS Lett. **281:**77–80.
51. **Weber, I. T., J. Wu, J. Adomat, R. W. Harrison, A. R. Kimmel, E. M. Wondrak, and J. M. Louis.** 1997. Crystallographic analysis of human immunodeficiency virus 1 protease with an analog of the conserved CA-p2 substrate—interactions with frequently occurring glutamic acid residue at P2′ position of substrates. Eur. J. Biochem. **249:**523–530.
52. **Williams, T., and C. Kelley.** 1998. GNUPLOT 1986–1993. [Online.] http://www.gnuplot.info.
53. **Wlodawer, A., M. Miller, M. Jaskolski, B. K. Sathyanarayana, E. Baldwin, I. T. Weber, L. M. Selk, L. Clawson, J. Schneider, and S. B. H. Kent.** 1989. Conserved folding in retroviral proteases: crystal structure of a synthetic HIV-1 protease. Science **245:**616–621.
54. **Wlodawer, A., and J. Vondrasek.** 1998. Inhibitors of HIV-1 protease: a major success of structure-assisted drug design. Annu. Rev. Biophys. Biomol. Struct. **27:**249–284.
55. **Zhang, Y., H. Qian, Z. Love, and E. Barklis.** 1998. Analysis of the assembly function of the human immunodeficiency virus tpe 1 Gag protein nucleocapsid domain. J. Virol. **72:**1782–1789.
56. **Zhang, Y.-M., H. Imamichi, T. Imamichi, H. C. Lane, J. Falloon, M. B. Vasudevachari, and N. P. Salzman.** 1997. Drug resistance during indinavir therapy is caused by mutations in the protease gene and in its Gag substrate cleavage sites. J. Virol. **71:**6662–6670.